Graphite deposit types, their origin, and economic significance

George J. Simandl[1, 2, a], Suzanne Paradis[3], and Carlee Akam[1]

[1] British Columbia Geological Survey, Ministry of Energy and Mines, Victoria, BC, V8W 9N3
[2] School of Earth and Ocean Sciences, University of Victoria, Victoria, BC, V8P 5C2
[3] Geological Survey of Canada, Pacific Division, Sidney, BC, V8L 4B2
[a] corresponding author: george.simandl@gov.bc.ca

Recommended citation: Simandl, G.J., Paradis, S., and Akam, C., 2015. Graphite deposit types, their origin, and economic significance. In: Simandl, G.J. and Neetz, M., (Eds.), Symposium on Strategic and Critical Materials Proceedings, November 13-14, 2015, Victoria, British Columbia, British Columbia Ministry of Energy and Mines, British Columbia Geological Survey Paper 2015-3, pp. 163-171.

1. Introduction

Graphite is an opaque, gray-black, and soft (1-2 on Mohs hardness scale) mineral with a metallic luster. It is characterized by a greasy feel, low density (2.09-2.23 g/cm^3), high resistance to thermal shock, and high electrical conductivity (Anthony et al., 2003). Inertness, compressibility, elasticity, and lubricity are other important physical properties (Wissler, 2006). The 2014 world natural graphite production was estimated at 1.17 million tonnes (Fig. 1; Olson, 2015), with most of it originating in China (67%), India (15%), Brazil (7%), Canada (3%), Turkey (3%), and North Korea (3%). Globally, most natural graphite is used in electrodes, refractories, lubricants, foundries, batteries, graphite shapes, recarburising, steelmaking, and friction products such as brake linings (Fig. 2; Shaw, 2013). Prices of selected products are shown in Table 1.

Refractory and high-technology applications make graphite a critical material in industrialized countries. High-technology uses of graphite represent a portion of the market with fastest forecasted growth.

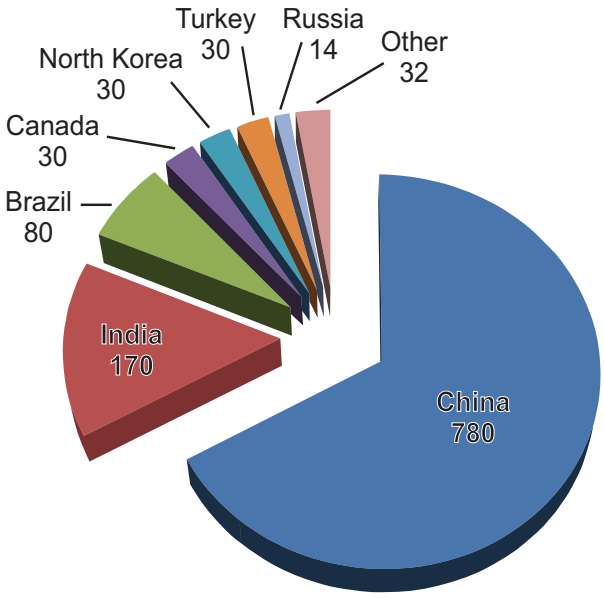

Fig. 1. Global graphite production, in thousands of tonnes, totalling 1.17 million tonnes, for 2014. Based on data from Olson (2015).

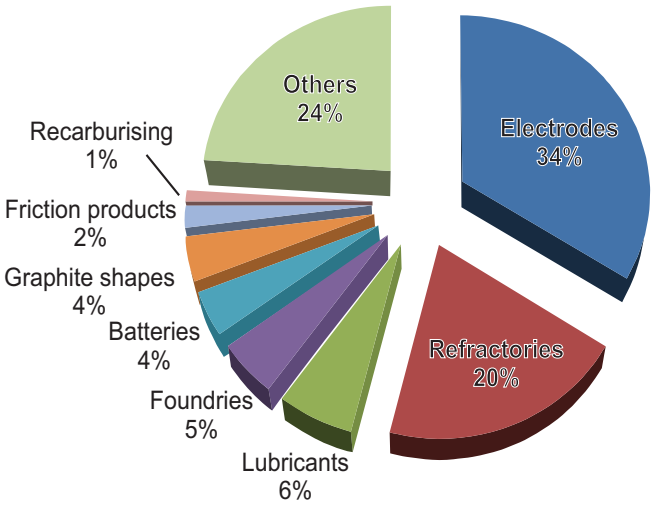

Fig. 2. Main uses of graphite for 2012. Based on data from Shaw (2013).

Examples of high-technology applications are: lithium-ion batteries for electric motor vehicles; large-scale electric energy storage devices; and graphite derivatives such as graphene (Sadasivuni et al., 2014; Dickson, 2014), spherical graphite, expanded graphite, and graphite foil. Graphene (sensu stricto) is a tightly packed layer of carbon atoms, one atom thick, bonded together in a hexagonal, honeycomb-like lattice, the stacking of which forms the graphite structure. Because of its potential uses in displays, conductive inks, composite materials, coatings and paints, electronics, energy generation, energy containers, membranes, 3D printers, sensors, photonics and optics, medicine, lubricants, and spintronics, graphene is considered to be a 'wonder material' (Mertens, 2015). Graphene-related research has received strong government financial support in many industrialized countries (Anonymous, 2015; Chiu, 2015; Hughes, 2015; Spasenovic, 2015). Spherical graphite is a product originally developed for use in lithium-ion batteries. It

Table 1. Prices of selected graphite products in US$/tonne. The purity of concentrate and, for some applications, size of crystalline flake are two key parameters. Abbreviations: FOB, free on board; CIF, Cost of Insurance and freight included; FCL, Full Container Load; ex-works, direct from the factory, excluding delivery costs, distribution costs, commission. Sources of data are: [a] Sawlan (2015), [b] Industrial Minerals (2015), and [c] Moores (2015).

	US$/tonne
Vein (lump and chip)[a]	
99.1% C, +1 mesh (>25.4mm), FOB Sri Lanka	2800
93% C, +60 mesh, FOB Sri Lanka	1550
Amorphous graphite[b]	
80-85% C, -200 mesh, China, FCL, CIF European port	430-480
Ore, 70-75% C, ex-works Austria	500-550
Flake graphite[b]	
85-87% C, +100 mesh -80mesh, FCL, CIF European port	700-800
90% C, +100 mesh -80 mesh, FCL, CIF European port	850-950
94-97% C, -100 mesh, FCL, CIF European port	900-950
90% C, +80 mesh, CIF, European port	950-1050
94-97% C, +100 mesh -80 mesh, FCL, CIF European port	1050-1150
94-97% C, +80 mesh, FCL, CIF European port	1200-1300
Spherical graphite[c]	7000-10000
Synthetic graphite[b]	
97-98%, CIF Asia	950-1450
98-99% CIF Asia	1000-1500
99.95% C, Switzerland	7000-20000

can be either synthetic or derived from crystalline flake graphite concentrate by processing that involves milling, physical rounding, purification, and surface treatment (Herstedt et al., 2003; Wu et al., 2006; Wang et al., 2008; Shaw, 2013). It takes approximately 100 kg of crystalline flake graphite concentrate (95% C) to produce 30 kg of spherical graphite assaying 99.9% C (Shaw, 2013). This is enough to produce a battery for one electric vehicle. Batteries are projected to account for approximately 5% of the global graphite production by 2016 (Shaw, 2013). In this application, spherical graphite derived from crystalline flake concentrate competes with its synthetic counterpart in terms of availability, price, and technical characteristics. Expanded graphite is another product derived from crystalline flake graphite. It is produced by intercalation with sulphuric and nitric acids (i.e., insertion of non-graphite atoms between graphite sheets) followed by expansion triggered by rapid temperature increase.

Worldwide, over 70 graphite exploration and development projects are being promoted, most of which are in Canada (see Lismore-Scott, 2014; Salwan, 2014). Barring unforeseeable political, military, or economic interference, we do not expect a natural graphite deficit before 2020.

2. Geology of graphite deposits

Natural graphite deposits of economic interest are grouped into three main categories: 1) microcrystalline; 2) vein graphite (lump and chip); and 3) crystalline flake graphite (Fig. 3). Deposit profiles by Simandl and Keenan (1998 a,b,c) provide an introduction to the main deposit types for exploration geologists and prospectors.

2.1. Microcrystalline graphite deposits

Commercially, microcrystalline graphite is referred to as ‘amorphous graphite’. This term is a misnomer because graphite has a crystal structure (readily detected by X-ray diffraction and Raman spectroscopy), which is lacking in truly

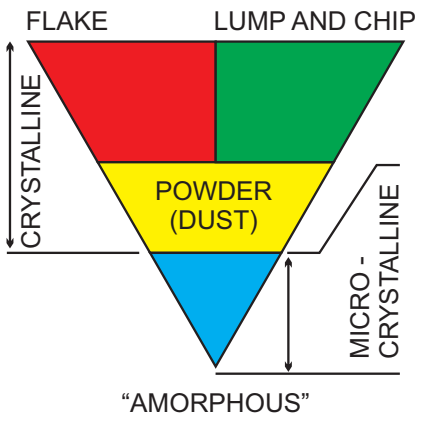

Fig. 3. Main categories of natural graphite currently available on the market. Modified from Simandl et al. (1995).

amorphous materials. In the scientific community, partially ordered graphite is referred to as 'semi-graphite' (Kwiecinska and Petersen, 2004) or, more recently, 'graphitic carbon' (Beyssac and Rumble, 2014).

Most microcrystalline graphite deposits are formed by sub-greenschist to greenschist contact metamorphism or regional metamorphism of coal seams (Taylor, 2006). Microcrystalline deposits consist mainly of small graphite particles intergrown with impurities. Typical deposits are stratiform or lens-shaped; beds may be deformed and/or repeated by folding and faulting. Pinching and swelling of beds is common. Deposits may consist of several beds, each up to a few metres thick. They may be exposed for hundreds of metres along strike. The ore contains from 30 to 95% graphite and, in many cases, more than 80%. Most mines producing microcrystalline graphite enrich ores only by hand sorting and milling. The product is sold mainly as forging lubricants and for applications where high ash content and low crystallinity is acceptable or preferred. An exception is the Kaiserberg deposit in Austria, where 92% graphite concentrate consisting of 2 micron size particles is produced (Taylor, 2006).

2.2. Vein graphite deposits

The most economically significant vein-type graphite deposits are found in the same metasedimentary belts as crystalline flake graphite deposits (see below), which are metamorphosed to upper amphibolite and granulite facies. In these belts, vein graphite deposits are found in skarn-type assemblages adjacent to igneous intrusions, in igneous intrusions, and in zones with a retrograde overprint (Simandl, 1992). Graphite veins are currently mined only in Sri Lanka, where graphite is extracted mainly by underground mining methods, routinely to depths in excess of 600 metres. The thickness of individual or anastomosing veins varies from a few millimetres to over one metre, but most are less than 0.3 metres. Other graphite-filled open spaces form pods and lenses, irregular bodies, stockworks, and saddle reefs (Simandl, 1992; Simandl and Keenan, 1998b). Rosettes, coarse flakes, fibers or needles oblique or perpendicular to wall rock and, in some cases, schistosity subparallel to the vein walls are characteristic textures. Outside of upper amphibolite to granulite facies metamorphic terrains and related intrusives (e.g., Cirkel, 1907), graphite veins, breccias, and stockworks also cut a variety of mafic and ultramafic rocks (e.g., Strens, 1965; Barrenechea et al., 1997; Crespo et al., 2006).

Vein graphite product (nearly monomineralic), graphite-rich fragments that are typically 0.5 to 0.8 cm in diameter are commercially referred to as 'lump' and 'chip' graphite, although 'lump' graphite may be much coarser (Table 1).

Pre-2009 disruptions in the supply of chip and lump graphite due to unrest in Sri Lanka forced the refractory industry to switch from vein-derived graphite to crystalline flake graphite. Once this transition was made, vein deposits lost their economic prominence as the source of graphite for refractories.

2.3. Crystalline flake graphite deposits

Disseminated graphite flakes are in a variety of rocks including marble, paragneiss, iron formation, quartzite, pegmatite, syenite (Simandl, 1992; Simandl et al., 1995) and, in extremely rare cases, serpentinized ultramafic rocks (e.g., Crespo et al., 2006). By far the most common hosts for economically significant crystalline flake deposits are paragneiss and marble that have been subjected to upper amphibolite to granulite facies metamorphism. Graphite deposits consisting of thick sequences of paragneiss are evenly mineralized and generally grade 2-3% graphite or less. A typical example is the Bissett Creek deposit in western Ontario (Fig. 4), which contains 69.8 million tonnes of measured and indicated resources grading 1.74% graphitic carbon (Cg) and 24 million tonnes of inferred resources grading 1.65% Cg (both at a 1.02% Cg cutoff grade; Northern Graphite Corporation, 2015). These resource estimates are not NI 43-101 compliant. The highest graphite grades in paragneiss-hosted deposits are along or near paragneiss-marble contacts, as exemplified by the Hartwell prospect, Quebec (Figs. 4 and 5). There, marble is separated from biotite gneiss by calcsilicate rocks (clinopyroxenites) and graphite-bearing scapolite paragneiss with graphite grades of 3-15% (Figs. 4 and 5). The contact between this graphite-rich unit and the biotite-gneiss is gradational and graphite content decreases with increasing distance from the calcsilicate rocks. Similarly, the high-grade Lac Knife deposit, in the Labrador Through (Quebec; Fig. 4), is also reported by Birkett et al. (1989), as cited by Saucier et al. (2012), to contain calcsilicate layers consisting mainly of scapolite. Measured and indicated resources at Lac Knife total 9,576,000 million tonnes grading 14.77% graphitic carbon, with inferred resources of 3,102,000 tonnes grading 13.25% carbon, using a cut-off grade of 3% graphitic carbon (Desautels et al., 2014). For some deposits (e.g., AA deposit, British Columbia; Fig. 4), the highest grade graphite is encountered in the crests of folds and is accompanied by retrograde minerals such as epidote and chlorite (Marchildon et al., 1993).

Marbles in terrains metamorphosed to granulite facies display a granoblastic texture and generally contain less than 0.5% crystalline flake graphite, although concentrations from 1 to 3% crystalline graphite are common. Graphite is regularly distributed throughout the host rock and the size of graphite flakes and calcite or dolomite crystals is directly correlated. Microscopic signs of corrosion or overgrowth on the graphite flakes that would indicate disequilibrium are lacking. Minor constituents such as diopside, magnesite, quartz, tremolite, fosterite, humite group minerals, garnets, scapolite, wollastonite, feldspar, phlogopite, muscovite, and serpentine account for less than 5% per volume of the rock.

Marbles with porphyroblastic texture are unusual. They contain from trace to 25% crystalline flake graphite. The best example is the historic Asbury graphite mine in Québec (Figs. 4 and 6). At this site, near-surface reserves were estimated to be 485,180 tonnes at 10.75% graphite (Séguin, 1974) and the mine was in production from 1980 to 1988 on seasonal basis.

Fig. 4. Location of Canadian graphite deposits discussed in the text.

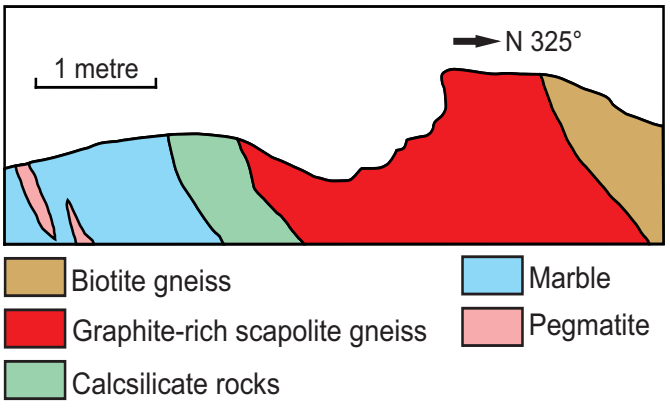

Fig. 5. Geological cross section of the Hartwell graphite prospect, Quebec. No vertical exaggeration. After Simandl et al. (1995).

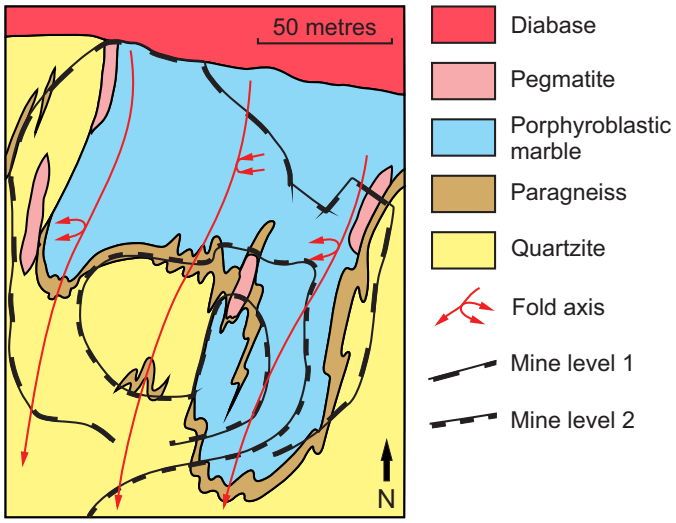

Fig. 6. Geological map of Asbury Graphite mine, Quebec. After Simandl et al. (1995).

Drilling in 1984, combined with a structural study, suggests additional resources at depth (Simandl, 1992). The graphite-rich porphyroblastic marble is calcitic and contains 2-10 mm clinopyroxene crystals. Other minerals, in concentrations less than 3%, are quartz, pyrite, garnet, titanite, magnetite, chlorite, and trace chalcopyrite, clinozoisite, and prehnite. Graphite flakes are dispersed throughout the ore, but concentrated around clinopyroxene crystals. Locally, graphite is observed as inclusions inside clinopyroxenes. Blue quartzite separates porphyroblatic graphite-rich marble from pale grey or white quartzite and indicates proximity to high-grade graphite mineralization. Obvious textural, mineralogical, or geochemical differences to explain the colour difference between the blue and white quartzites are absent. Although no primary fluid inclusions were identified in either quartzites, temperatures of homogenization and melting suggest the presence of CH_4, N_2, SO_4, or H_2S, in addition to CO_2. Limited Raman spectroscopy detected CO_2 with lesser concentrations of CH_4 and N_2 in fluid inclusions in blue quartzite (Simandl, 1992).

Most crystalline flake graphite deposits are mined in open pits. Typically, the ore is crushed, milled, processed using flotation and, depending on its physical properties and intended use, may be further processed. Crystalline flake graphite concentrate consists of flakes typically larger than 200 mesh (equivalent to 74 microns); fines produced during milling may be sold as graphite powder or dust.

Significant graphite concentrations in magnetite deposits are present in the Grenville Province (Raymond, 1978; Champigny, 1980; Gauthier and Brown, 1986; Simandl et al., 1995). Although none of these deposits are currently in production, some were mined for iron (e.g., Forsyth mine, Quebec). Several minor feldspar-rich intrusions (including pegmatites) cutting metasedimentary rocks contain up to 5%wt. graphite flakes, but are generally too restricted in size to be of economic interest (Simandl et al., 1995).

3. Origin of natural graphite deposits of economic interest

Natural graphite deposits of economic interest are most likely formed by: 1) the maturation and metamorphism of organic material; and 2) precipitation from C-O-H fluid (metamorphic or metasomatic) triggered by changes in temperature and pressure conditions, fluid buffering, or by mixing of C-O-H fluids of different compositions and probably different origins (for review, see Simandl, 1992).

3.1. Maturation and metamorphism of organic material

The transformation of immature organic material to graphite begins with carbonization and is followed by graphitization (Fig. 7). This is the generally accepted hypothesis to explain the origin of microcrystalline and low-grade crystalline flake graphite deposits. During the carbonization stage, organic substances are converted into carbon or carbon-containing residues, and oil and natural gas are released. Carbonization takes place during diagenesis, whereas graphitization takes place at higher temperatures and pressures of deeper burial and metamorphism. During both carbonization and graphitization, the atomic ratios of H/C and O/C systematically decrease (Fig. 7). Kerogens I, II, and III are derived largely from lacustrine algae (H/C > 1.25), marine microorganisms (1.1<H/C<1.5), and terrestrial plants (coal deposits; H/C<1), respectively. During the carbonization process, kerogens go from immature to oil and gas forming stages. The carbon-enriched residue stays in place, while liberated hydrocarbons are expelled. Further burial accompanied or followed by regional or contact metamorphism may result in graphitization of residual material (development of a well-ordered graphite crystal structure). Various stages and aspects of the kerogene-graphite transition are addressed by Grew (1974), Diessel and Offler (1976), Jones and Edison (1979), Oberlin et al. (1980), North (1985), Wopenka and Pasteris (1993), and Buseck and Beysasak (2014).

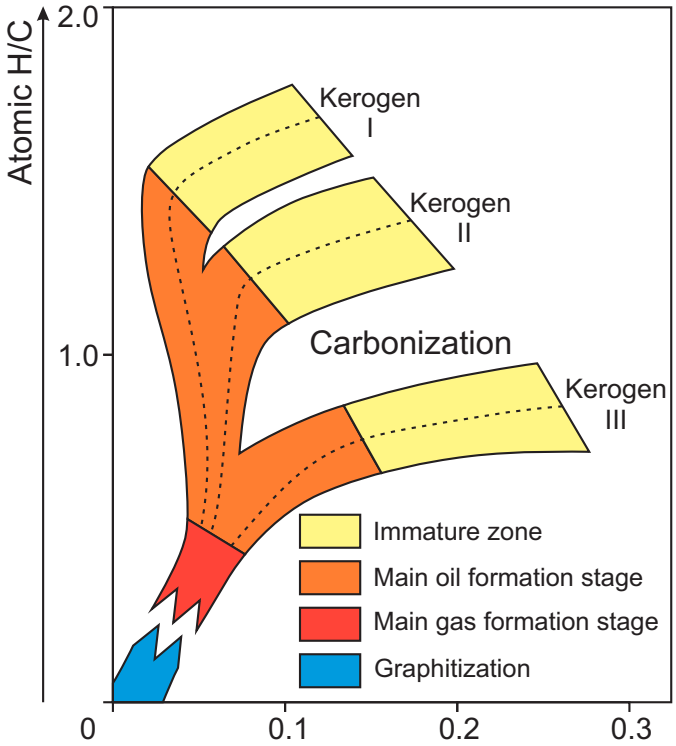

Fig. 7. Kerogen maturation in terms of H/C and O/C atomic ratios. Modified from Buseck and Beyssac (2014); based on data of Grew (1974), and Vandenbroucke and Largeau (2007).

3.2. Precipitation of graphite from C-O-H fluids

In contrast to the origin of microcrystalline and low-grade crystalline flake graphite deposits, the origin of graphite veins is still widely debated and the genesis of enrichment zones within crystalline flake graphite deposits (e.g., Hartwell prospect and Asbury Graphite deposit) remains largely overlooked. Ternary C-O-H diagrams (Figs. 8-10) offer a simple approach to explain the origin of high-grade graphite deposits that show open space features and textures such as breccia zones and veins, or enrichment zones in crystalline flake graphite deposits.

Graphite saturation curves on C-O-H ternary diagrams are temperature and pressure dependent (e.g., Holloway, 1984;

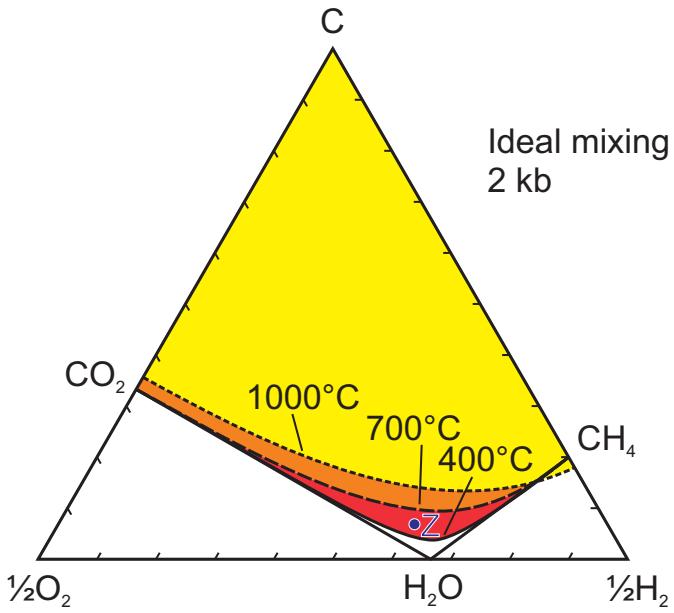

Fig. 8. Ternary C-O-H diagram showing increasing size of graphite stability field with decreasing temperatures from 1000º to 400°C for constant pressure of 2 kb, assuming ideal mixing according to Lewis and Randall Rule. Modified from Ferry and Baumgartner (1987).

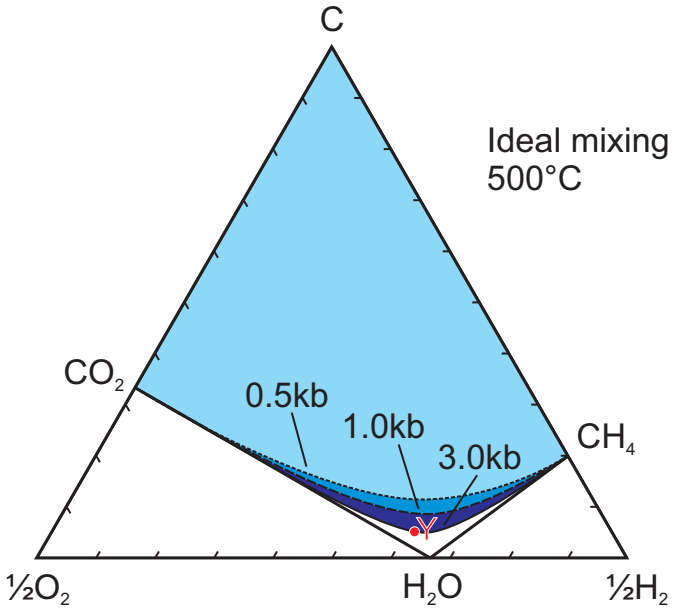

Fig. 9. Ternary C-O-H diagram showing increasing size of graphite stability field with increasing pressure from 0.5 to 3.0 kb for constant temperature of 500°C, assuming ideal mixing (Lewis and Randall Rule). Modified from Ferry and Baumgartner (1987).

Ferry and Baumgartner, 1987; Pasteris, 1999; Luque and Rodas, 1999; Huizenga, 2011; Huizenga and Touret, 2012). At constant pressure, the graphite stability field increases with decreasing temperature. For example, assuming a constant pressure of 2 kb, graphite can't precipitate from cooling of a C-O-H fluid of the composition Z at 1000ºC or 700°C, but will start to precipitate before the fluid cools below 400°C (Fig. 8). At constant temperature, the stability field of graphite increases with increasing pressure (Ferry and Baumgartner, 1987). For example, at 500°C graphite will not precipitate from a fluid of composition Y at pressures of 0.5 and 1.0 kb, but will precipitate at pressures of 3 kb or greater (Fig. 9).

Figure 10 shows part of the C-O-H ternary diagram at 600°C and pressure of 3.5 kb. A fluid of composition A plots within the graphite stability field. As graphite precipitates, the composition of the fluid evolves along the corresponding tie-line, as shown by the green arrow, towards the graphite saturation curve. Figure 10 also shows fluids of compositions B and F, both of which lie outside the graphite stability field. It would be impossible to precipitate graphite from either of these fluids alone. However, if we mix these two fluids, the composition of the resulting mixture will lie somewhere along the mixing line B-F. If a small quantity of fluid F is added to fluid B, then the composition of the resulting fluid will shift slightly to the right (e.g., point C). As more fluid F is added to the system, the composition of the resulting fluid will keep shifting to the right until point D is reached and the first crystal of graphite precipitates. As more fluid of composition F enters the system, the composition of the fluid follows the graphite saturation curve, passing through point E, and graphite keeps precipitating.

4. Discussion and summary

Microcrystalline graphite deposits form by maturation of organic material in sedimentary rocks (coal seams) followed by regional or contact metamorphism attaining sub-greenschist to greenschist facies. It is used mainly in greases and forging lubricants and has no known use in high-technology applications.

Economically minable graphite veins are typically hosted by sedimentary successions that have been subjected to granulite facies metamorphism and intruded by minor igneous bodies. Mining of graphite veins similar to those that are mined in Sri Lanka involves underground methods and is labor intensive. Graphite morphology, open-space filling textures, and thermodynamic models indicate that these veins originate by precipitation from C-H-O fluids.

Most exploration projects target crystalline flake deposits. Low concentrations of crystalline flake graphite in marbles and paragneisses probably result from maturation of organic material in precursor sediments, followed by graphitization at pressure and temperature conditions approaching or reaching granulite facies. Graphite-rich zones in disseminated crystalline flake deposits (e.g., Asbury Graphite mine in Quebec, AA deposit in British Columbia) are typically at or near marble-paragneiss contacts and in the crests of folds. These zones are characterized by porphyroblastic textures in marbles, skarn mineralogy at or near the contacts, and decreasing concentrations of scapolite in the paragneiss with increasing distance from the contacts. In these settings, graphite enrichment is likely the result of: a) mixing of fluids produced by decarbonation reactions in marbles and dehydration reactions in paragneiss, or fluids derived

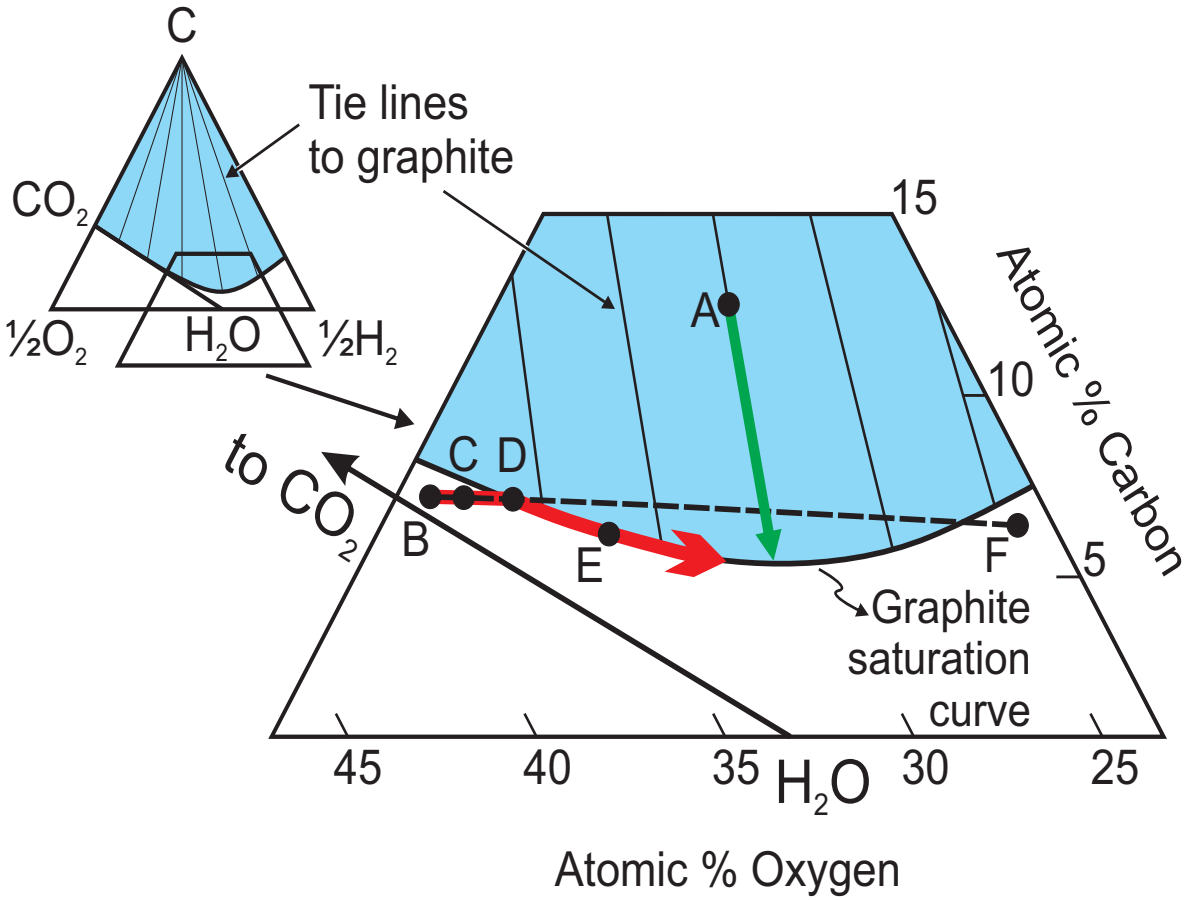

Fig. 10. Ternary C-O-H diagram at 600°C and 3.5 kb showing precipitation of graphite from the fluid of composition A (within the graphite stability field) and from mixing of fluids of composition B and F, both lying outside of the graphite stability field. Refer to detailed explanation in text. Modified from Rumble et al. (1982).

from pegmatites and other minor intrusions; or b) cooling of C-H-O fluids. Sub-granulite facies minerals (e.g., prehnite and clinozoisite) observed in some veins and high-grade portions of disseminated flake graphite deposits suggest post-metamorphic peak (retrograde) temperatures of formation.

Forecasted increase in use of natural graphite in high-technology applications turns graphite into a 'hot' commodity; however, fundamental technical and economic parameters of individual deposits have to be taken into consideration when prioritizing exploration and development targets. Enriched zones of crystalline flake graphite deposits are of particular interest to industrialized countries because they are mined by open pit methods (not labour intensive) and provide critical material for high-technology applications.

Acknowledgments

Comments and suggestions from Douglas Rumble III of the Geophysical Laboratory of the Carnegie Institution of Washington are greatly appreciated.

References cited

Anonymous, 2015. Graphene news review. Industrial Minerals, no. 571, 21-22.

Anthony, W., Bideaux, R.A., Bladh, K.W., and Nichols, M.C. (Eds.), 1990. Handbook of mineralogy, volume I: elements, sulfides, sulfosalts. Mineral Data Publishing, Tucson, Arizona, 588p.

Barrenechea, J.F., Luque, F.J., Rodas, M., Pasteris, J.D., 1997. Vein-type graphite mineralization in the Jurassic volcanic rocks of the external zone of the Betic Cordillera (southern Spain). The Canadian Mineralogist, 35, 1379-1390.

Beyssac, O., and Rumble, D., 2014. Graphitic carbon: a ubiquitous, diverse, and useful geomaterial. Elements, 10, 415-120.

Birkett, T., Godue, R., and Marchildon, N., 1989. The Knife lake graphite deposit, geology, mineralogy and mineral textures, 1989 field and laboratory investigations. Unpublished documents, Québec Géosciences Center.

Buseck, P., and Beyssac, O., 2014. From organic matter to graphite: graphitization. Elements, 10, 421-426.

Champigny, N., 1980. Stratigraphic relationship between iron formations and zinc mineralization, Mt. Laurier Basin, Quebec. Progress report to Riocanex Inc., Toronto, Ont., 15p.

Chiu, G., 2015. Perfection of the pursuit: the Canadian option for graphene's commercialisation. Industrial Minerals, no. 571, 25-26.

Cirkel, F., 1907. Graphite, its properties, occurrences, refining and uses. Canada Department of Mines, Mines Branch, Ottawa, No. 202, 263p.

Crespo, E., Luque, F.J., Rodas, M., Wada, H., and Gervilla, F., 2006. Graphite-sulfide deposits in Ronda and Beni Bouser peridotites (Spain and Morocco) and the origin of carbon in mantle-derived rocks. Gondwana Research, 9, 279-290.

Desautels, P., D'Anjou, N., Skiadas, N., Cassoff, J., Pengel, E., Bilodeau, M.L., and Buchanan, M.J., 2014. NI 43-101 technical report on the Lac Knife graphite feasibility study Quebec-Canada. Focus Graphite Inc., 293p. <http://www.focusgraphite.com/wp-content/uploads/largeReport/Lac-Knife-Feasibility-Study-Technical-Report-August-2014.pdf> Accessed July 15, 2015.

Dickson, J.S., 2014. Talga eyes graphene potential. Industrial Minerals, no. 567, 35-36.

Diessel, C.F.K., and Offler, R., 1976. The application of reflectance determination on coalified and graphitized plant fragments to metamorphic studies. Journal of the Geological Society of Australia, 23, 293-297.

Ferry, J.M., and Baumgartner, L., 1987. Thermodynamic models of molecular fluids at the elevated pressures and temperatures of crustal metamorphism. In: Carmichael, I.S.E., and Eugster, H.P., (Eds.), Thermodynamic Modeling of Geological Materials: Minerals, Fluids and Melts. Mineralogical Society of America Reviews in Mineralogy, Volume 17, pp. 323-365.

Grew, E.S., 1974. Carbonaceous material in some metamorphic rocks of New England and other areas. Journal of Geology, 82, 50-73.

Gauthier, M., and Brown, A.C., 1986. Zinc and iron metallogeny in the Maniwaki-Gracefield district, southwestern Quebec. Economic Geology, 81, 89-112.

Herstedt, M., Fransson, L., and Edström, K., 2003. Rate capability of natural Swedish graphite as anode material in Li-ion batteries. Journal of Power Sources, 124, 191-196.

Holloway, J.R., 1984. Graphite-CH_4-H_2O-CO_2 equilibria at low grade metamorphic conditions. Geology, 12, 455-458.

Hughes, E., 2015. The importance of Manchester's "Graphene City". Industrial Minerals, no. 571, 27-28.

Huizenga, J.-M., 2011. Thermodynamic modelling of a cooling C-O-H fluid-graphite system: implications for hydrothermal graphite precipitation. Mineralium Deposita, 46, 23-33.

Huizenga, J.-M., and Touret, J.L.R., 2012. Granulites, CO_2 and graphite. Gondwana Research, 22, 799-809.

Industrial Minerals, 2015. Graphite Prices. <http://www.indmin.com/Graphite.html> Accessed March 26, 2015.

Jones, R.W., and Edison, T.A., 1979. Integration of microscopic organic analysis and geochemical measurements in evaluation of source rocks. American Association of Petroleum Geologists, Bulletin 63, p.476.

Kwiecińska, B., and Petersen, H.I., 2004. Graphite, semi-graphite, natural coke, and natural char classification—ICCP system. International Journal of Coal Geology, 57, 99-116.

Lismore-Scott, S.L., 2014. Graphite projects and reserves – are we facing an oversupply situation? Industrial Minerals, no. 567, 29-32.

Luque, F.J., and Rodas, M., 1999. Constraints on graphite crystallinity in some Spanish fluid-deposited occurrences form different geologic settings. Mineralium Deposita, 34, 215-219.

Marchildon, N., Simandl, G.J., and Hancock, K.D., 1993. The AA graphite deposit, Bella Coola area, British Columbia: exploration implications for the coast plutonic complex. In: Geological Fieldwork 1992, British Columbia Ministry of Energy and Mines, British Columbia Geological Survey Paper 1993-1, 389-397.

Mertens, 2015. The graphene handbook. Lulu.com, Raleigh, North Carolina, 2nd edition, 136p. <http://www.graphene-info.com/handbook/> Accessed August 12, 2015.

Moores, S., 2015. Battery grade graphite set for record year. Mining.com <http://www.mining.com/web/battery-grade-graphite-set-for-record-year/> Accessed July 22, 2015.

North, F.K., 1985. Petroleum Geology. Allen & Unwin, Boston, 605p.

Northern Graphite Corporation, 2015. Bissett Creek Project. <http://northerngraphite.com/bissett-creek-project/> Accessed June 30, 2015.

Oberlin, A., Boulmier, J.L., and Villey, M., 1980. Electron microscopic study of kerogen microtexture. Selected criteria for determining the evolution path and evolution stage of kerogen. In: Durand, B., (Ed.), Kerogen. Editions Technip, Paris, pp. 191-241.

Olson, D.W., 2015. Graphite (Natural). U.S. Department of the Interior, U.S. Geological Survey, Mineral Commodity Summaries, January 2015, pp.68-69. <http://minerals.usgs.gov/minerals/pubs/mcs/2015/mcs2015.pdf> Accessed June 30, 2015.

Pasteris, J.D., 1999. Causes of the uniformly high crystallinity of graphite in large epigenetic deposits. Journal of Metamorphic Geology, 17, 779-787.

Raymond, D., 1978. Etude de deux indices minéralisés (magnetite) du Canton de Cameron, Comté de Gatineau, Québec. Unpublished BSc Thesis, Ecole Polytechnique de Montréal, Montréal, 65p.

Rumble, D., Ferry, J.M., Hoering, T.C., and Boucot, A.J., 1982. Fluid flow during metamorphism at the Beaver Brook fossil locality, New Hampshire. American Journal of Science, 282, 886-919.

Salwan, S., 2014. The Indian graphite industry – why we need to take notice. Industrial Minerals, no. 567, 32-34.

Salwan, S., 2015. Vein graphite prices resist market slump. Industrial Minerals. <http://www.indmin.com/Article/3471988/Graphite/Vein-graphite-prices-resist-market-slump.html> Accessed July 22, 2015.

Saucier, G., Lyons, E., and Baril, F., 2012. NI 43-101 technical report on the Lac Knife graphite project. Focus Metals Inc., 87p. <www.focusgraphite.com/french/wp-content/uploads/2012/07/43-101Report_Lac-Knife.pdf> Accessed July 10, 2015.

Séguin, E., 1974. Preliminary report on the projected operation of a graphite mine at Notre-Dame-du-Laus, Québec. Somex Ltd., 16p.

Shaw, S., 2013. Graphite demand and growth: the future of lithium-ion batteries in EVs and HEVs. Proceedings of 37th ECGA General Assembly. <http://www.saintjeancarbon.com/files/2513/7157/3343/Graphite_demand_Li-ions_April_2013.pdf> Accessed June 30, 2015.

Simandl, G.J., 1992. Gîtes de graphite de la région de la Gatineau, Québec. Unpublished Ph.D. thesis, Université de Montréal, Montréal, Canada, 383p.

Simandl, G.J., and Keenan, W.M., 1998a. Microcrystalline graphite. In: Geological Fieldwork 1997, British Columbia Ministry of Energy and Mines, British Columbia Geological Survey Paper 1998-1, 24O-1-24O-3. <http://www.empr.gov.bc.ca/Mining/Geoscience/PublicationsCatalogue/Fieldwork/Documents/1997/simandl_kenan_po3.pdf> Accessed June 30, 2015.

Simandl, G.J., and Keenan, W.M., 1998b. Vein graphite in metamorphic terrains. In: Geological Fieldwork 1997, British Columbia Ministry of Energy and Mines, British Columbia Geological Survey Paper 1998-1, 24Q-1-24Q-3. <http://www.empr.gov.bc.ca/Mining/Geoscience/PublicationsCatalogue/Fieldwork/Documents/1997/simandl_kenan.pdf> Accessed June 30, 2015.

Simandl, G.J., and Keenan, W.M., 1998c. Crystalline flake graphite. In: Geological Fieldwork 1997, British Columbia Ministry of Energy and Mines, British Columbia Geological Survey Paper 1998-1, 24P-1-24P-3. <http://www.empr.gov.bc.ca/Mining/Geoscience/PublicationsCatalogue/Fieldwork/Documents/1997/simandl_kenan_po4.pdf> Accessed June 30, 2015.

Simandl, G.J., Paradis, S., Valiquette, G., and Jacob, H.L., 1995. Crystalline graphite deposits, classification and economic potential. Proceedings of 28th Forum on the Geology of Industrial Minerals, Marinsburg, West Virginia, May 3-8, 1992, pp.168-174.

Spasenovic, M., 2015. Leavin lab status: Graphene's various routes to industrial application. Industrial Minerals, no. 571, 23-25.

Strens, R.G.T., 1965. The graphite deposits of Seathwaite in Borrowdale, Cumberland. Geological Magazine, 102, 393-406.

Sadasivuni, K.K., Ponnamma, D., Thomas, S., and Grohens, Y., 2014. Evolution from graphite to graphene elastomer composites. Progress in Polymer Science, 39, 749-780.

Taylor, H.A., Jr., 2006. Graphite. In: Kogel, J.E., Trivedi, N.C.,

Barker, J.M., and Krukowski, W.T., (Eds.), Industrial Minerals and Rocks. Society for Mining, Metallurgy, and Exploration, Inc., Littleton, Colorado, pp. 507-518.

Vandenbroucke, M., and Largeau, C., 2007. Kwerogen origin, evolution and structure. Organic Geochemistry, 38, 719-833.

Wang, X., Gai, G.-S., Yang, Y.-F., and Shen, W.-C., 2008. Preparation of natural microcrystalline graphite with high spericity and narrow size distribution. Powder Technology, 181, 51-56.

Wissler, M., 2006. Graphite and carbon powders for electrochemical applications. Journal of Power Sources, 156, 142-150.

Wopenka, B., and Pasteris, J.D., 1993. Structural characterization of kerogens to granulite-facies graphite: applicability of Raman microprobe spectroscopy. American Mineralogist, 78, 533-557.

Wu, Y.-S., Wang, Y.-H., and Lee, Y.-H., 2006. Performance enhancement of spherical natural graphite by phenol resin in lithium ion batteries. Journal of Alloys and Compounds, 426, 218-222.